Supplementary Information (SI) for Reaction Chemistry & Engineering.
This journal is © The Royal Society of Chemistry 2025

Electronic Supplementary Information

Facile Room-Temperature Synthesis of Hydroxyl Sulfides for Efficient Oxygen Evolution Reaction

Pei-Wei Zhong[1], Hong-Xiao Yang[1], Wenkang Xu, Zhiyang Yu, Bei Li, Hongjuan Wang, Yonghai Cao, Hao-Fan Wang* and Hao Yu*

School of Chemistry and Chemical Engineering, South China University of Technology, Guangzhou 510641, Guangdong, China.

E-mail addresses: whf@scut.edu.cn; yuhao@scut.edu.cn

Text S1. Chemicals and reagents

The chemical reagents used in this experimental study were all analytical-grade reagents and could be used directly according to the received standards without further purification. Ferric nitrate nonahydrate ($Fe(NO_3)_3 \cdot 9H_2O$, 99.9%) was purchased from Shanghai Macklin Biochemical Co., Ltd. Sodium sulfide nonahydrate ($Na_2S \cdot 9H_2O$, 98.0%) was obtained from Shandong Keyuan Biochemical Co., Ltd. Nickel foam (Ni foam, 99.7%) was supplied by Guangdong Zhuguang New Energy Technology Co., Ltd. Commercial ruthenium dioxide (RuO_2 99.9%) was acquired from Strem Chemicals. Acetone (C_2H_6O 99%) was purchased from Shanghai Aladdin Biochemical Technology Co., Ltd. Hydrochloric acid (HCl AR) was sourced from Guangdong Guangshi Reagent Technology Co., Ltd. Nafion binder (Nafion 5%) was obtained from DuPont. Anhydrous ethanol (C_2H_6O 99.7%) and isopropanol (C_3H_8O 99%) were purchased from Tianjin Damao Chemical Reagent Factory. Deionized water used in experiments were prepared using an ultrapure water system in our laboratory.

Text S2. The preparation of RuO_2 catalysts

Accurately weigh 5 mg of commercial RuO_2 powder, then add 50 μL of Nafion solution, 150 μL of ultrapure water, and 800 μL of isopropanol. After mixing, the resulting suspension is treated in an ultrasonic cleaner for 45 minutes to ensure the formation of a homogeneous catalyst ink. The well-dispersed ink is then drop-cast onto the surface of a 1 cm^2 nickel foam using a micropipette. The sample is subsequently dried rapidly under an infrared lamp. Once the solvent has completely evaporated, the uniformly black-coated NF is obtained as the RuO_2/NF catalyst.

Text S3. Synthesis and sulfurization mechanism of NiFe-LDH precursors

To investigate the transformation mechanism from hydroxide precursors to multi-anionic structures, nickel foam (NF) was employed as the substrate, and Fe^{3+} ions were introduced to construct NiFe-LDH/NF. Subsequently, a room-temperature sulfuration reaction was carried out to synthesize the target material, S-NiFe-LDH/NF. Due to the

hydrolysis of Fe^{3+}, the pH of a 0.2 M $Fe(NO_3)_3$ solution is only 1.2.[1] On the surface of nickel powder immersed in this solution, the following redox half-reactions may occur:[2]

$$NO_3^- + 2H^+ + 2e^- \rightleftharpoons NO_2^- + H_2O \qquad E_1^o = +0.934\ V \qquad Eq.\ S1$$

$$Fe^{3+} + e^- \rightleftharpoons Fe^{2+} \qquad E_2^o = +0.771\ V \qquad Eq.\ S2$$

$$2H^+ + 2e^- \rightleftharpoons H_2 \qquad E_3^o = 0\ V \qquad Eq.\ S3$$

$$Ni^{2+} + 2e^- \rightleftharpoons Ni \qquad E_4^o = -0.25\ V \qquad Eq.\ S4$$

Based on the standard electrode potentials of the relevant reactions, metallic nickel (Ni^0), which is a reducing species, can be oxidized in $Fe(NO_3)_3$ solution, releasing Ni^{2+} ions into the solution. This oxidation process consumes H^+, leading to an increase in the local pH near the Ni^0 surface, which in turn promotes the deposition of hydroxides. The overall reaction can be divided into three main stages: In the initial stage, Ni^0 reacts with NO^{3-}, H^+, and Fe^{3+}, undergoing oxidation and releasing Ni^{2+} into the solution—this is referred to as the etching process. During this stage, the reactions between nickel and both nitrate and protons consume H^+, creating a localized alkaline environment at the Ni surface. In the second stage, as the local pH near the Ni^0 surface increases, amorphous metal hydroxides begin to precipitate on the nickel substrate, forming a coating on the nickel particles. Considering the solubility product constants (K_{sp}) of $Fe(OH)_3$ (2.79×10^{-39}), $Ni(OH)_2$ (5.48×10^{-16}), and $Fe(OH)_2$ (5.48×10^{-17}), and given the initially high concentration of Fe^{3+} and its extremely low K_{sp}, Fe^{3+} preferentially precipitates first to form an alpha-FeO_xH_y layer on the Ni surface. In the final stage, the reaction between Ni^0 and NO^{3-} continues, further increasing the concentrations of Ni^{2+} and pH near the Ni^0 surface. At this point, both Ni^{2+} and Fe^{3+} co-precipitate on the nickel surface, forming an alpha-$NiFeO_xH_y$ layer.[3] Due to its amorphous and porous nature, the alpha-$NiFeO_xH_y$ layer allows NO^{3-} and H^+ to penetrate through and continue oxidizing the underlying Ni^0, thereby driving the progressive growth of the alpha-$NiFeO_xH_y$ layer. Therefore, by simply immersing NF in an Fe^{3+} solution at room temperature, nickel–iron layered double hydroxide (NiFe-LDH/NF) can be formed. Notably, in our experiments, a 0.2 M $Fe(NO_3)_3$ solution severely corrodes the Ni foam,

compromising its integrity. Therefore, a 50 mM solution was employed in this work.

Text S4. Preparation for electrochemical measurement

Electrochemical measurements were conducted using a standard three-electrode setup. The working electrode was prepared by directly using or modifying NF with different catalysts. A graphite rod and a Hg/HgO electrode served as the counter and reference electrodes, respectively. Prior to measurements, the reference electrode was calibrated against the reversible hydrogen electrode (RHE) by recording the LSV curve of commercial Pt/C in hydrogen-saturated 1.0 M KOH. Electrochemical data were recorded using a CHI760E workstation (Shanghai Chenhua Instruments Co., Ltd.) and a VersaSTAT4 system (Princeton Applied Research).

Text S5. Analysis and characterizations

X-ray diffraction (XRD) measurements were conducted using a Miniflex 600 diffractometer (Rigaku), employing a Cu target with Kα radiation (λ = 0.15406 nm). The scan step size was set to 0.01°, with a sampling interval of 0.05 s. Scanning electron microscopy (SEM) was performed using a Zeiss Merlin high-resolution field emission SEM at an accelerating voltage of 5 kV. High-resolution transmission electron microscopy (HRTEM) analysis was carried out on JEM 1400 Plus and JEM 2100F instruments (JEOL), equipped with a QUANTAX energy-dispersive X-ray spectroscopy (EDS) system (Bruker). X-ray photoelectron spectroscopy (XPS) measurements were conducted using a K-Alpha+ spectrometer (Thermo Fisher Scientific). Energy calibration was performed using the C 1*s* peak at 284.80 eV. Fourier-transform infrared spectroscopy (FTIR) was performed on a Nicolet IS50 spectrograph.

Supplementary figures

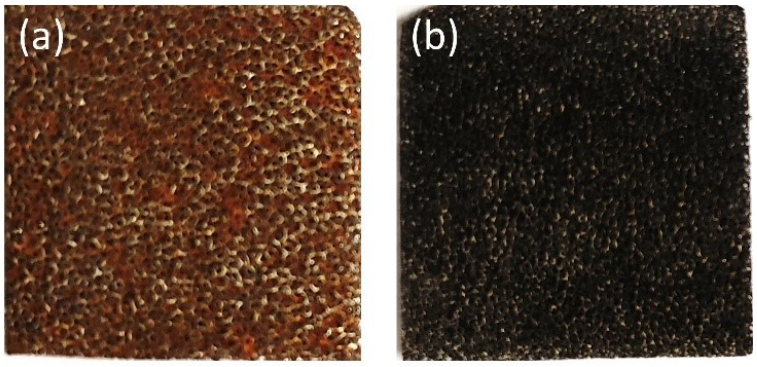

Fig. S1 Photographs of catalysts: (a) NiFe-LDH/NF and (b) S-NiFe-LDH/NF.

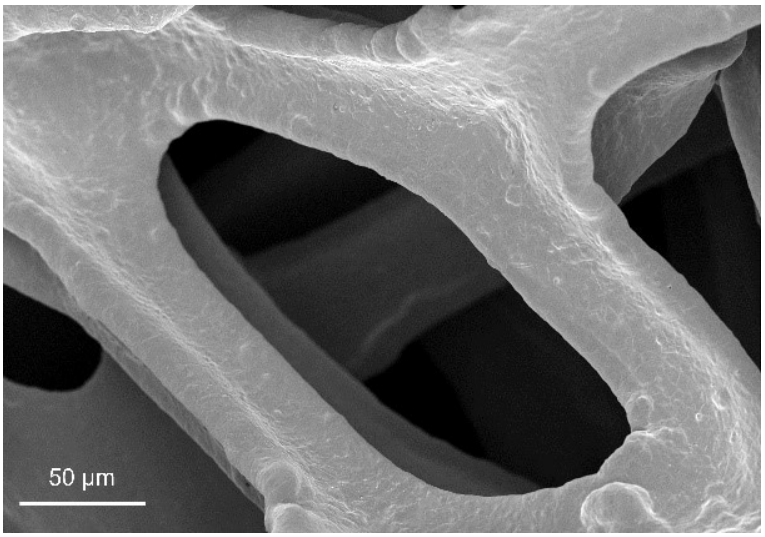

Fig. S2 The SEM image of NF.

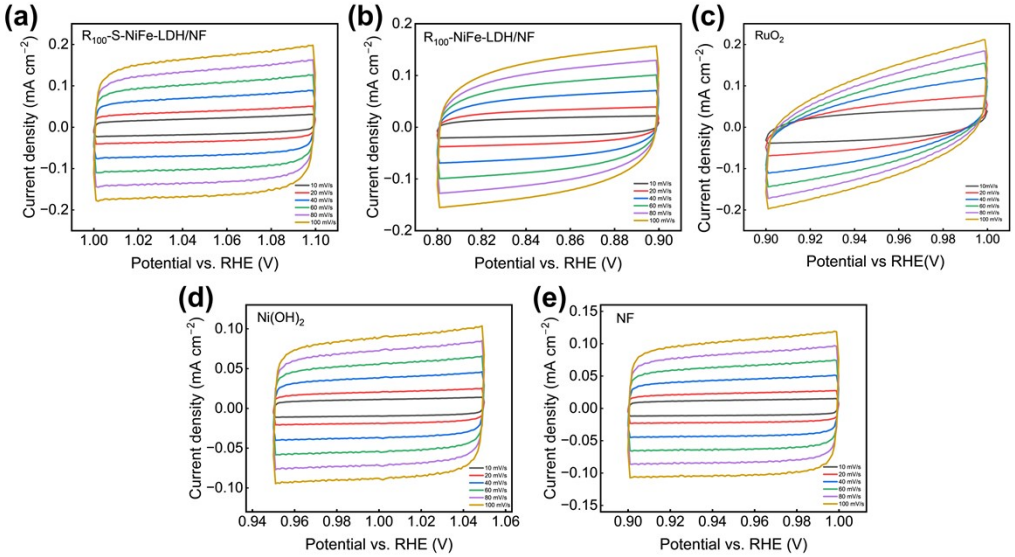

Fig. S3 CV curves of (a) R_{100}-S-NiFe-LDH/NF, (b) R_{100}-NiFe-LDH/NF, (c) RuO_2, (d) $Ni(OH)_2$ and (e) NF in 1.0 M KOH, with the scan rate increasing from 10 mV s^{-1} to 100 mV s^{-1}.

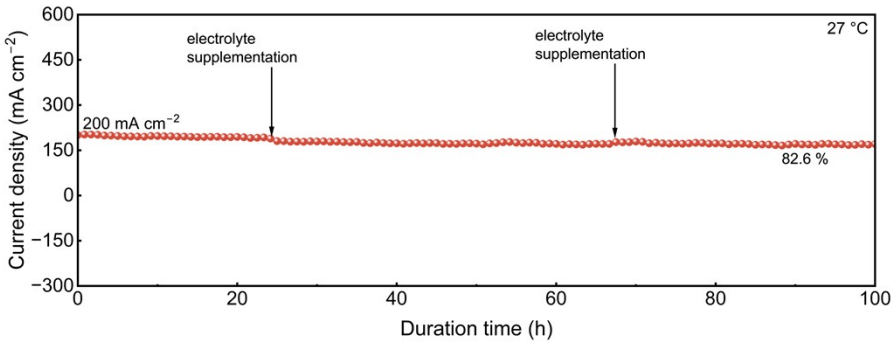

Fig. S4 The *i-t* curve of R_{100}-NiFe-LDH/NF at an initial current density of 200 mA cm^{-2}.

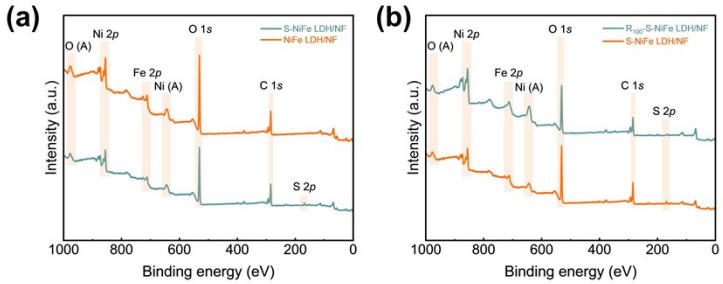

Fig. S5 XPS survey spectrum of (a) NiFe-LDH/NF and S-NiFe-LDH/NF; (b) S-NiFe-LDH/NF and R_{100}-S-NiFe-LDH/NF.

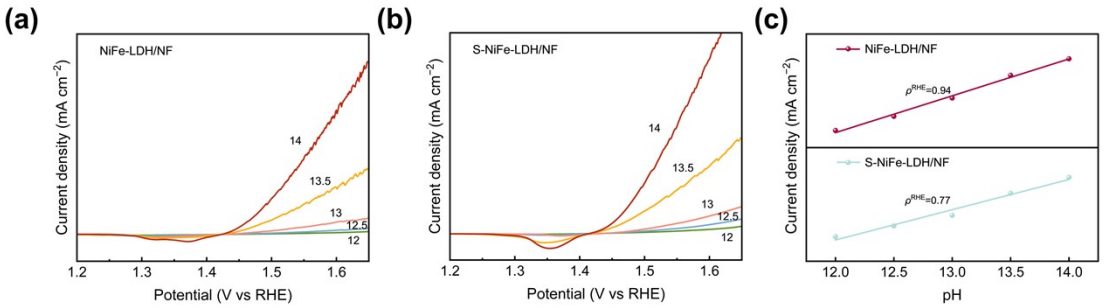

Fig. S6 (a) LSV curves of NiFe-LDH/NF and (b) S-NiFe-LDH/NF recorded at pH 12.5, 13.0, 13.5, and 14. (c) Logarithmic dependence of the OER current density on pH at 1.60 V (vs. RHE). The numerical values shown in the figure correspond to the proton reaction order ρ ($\rho^{\mathrm{RHE}} = \partial \log j / \partial \mathrm{pH}$).

Tab. S1. XPS elemental composition of the S-NiFe-LDH/NF sample

Element	Atomic %
C	44.55
O	39.48
Ni	8.93
Fe	4.06
S	2.98

1. C. M. Flynn, Jr., *Chemical Reviews*, 1984, **84**, 31-41.
2. Y. H. Chen, X. H. Zeng, Q. Meyer, C. Zhao, Z. J. He, F. X. Wu, H. L. Tang and Y. Cheng, *Electrochimica Acta*, 2023, **442**, 141862.
3. B. L. Lan, B. Shao, F. J. Yang, W. Pang, Z. P. Guo, T. Meng, Z. Zhang and J. Huang, *Small Structures*, 2022, **3**, 2200085.